

Mathematical Architecture of Approximate Deconvolution Models of Turbulence*

A. Labovschii¹, W. Layton², C. Manica³, M. Neda⁴, L. Rebholz⁵, I. Stanculescu⁶, and C. Trenchea⁷

¹ Department of Mathematics, University of Pittsburgh, Pittsburgh, PA, ayl2@pitt.edu

² Department of Mathematics, University of Pittsburgh, Pittsburgh, PA, wjl1@pitt.edu

³ Departamento de Matemática Pura e Aplicada, Federal University of Rio Grande do Sul, Porto Alegre-RS-Brazil, cac15@pitt.edu

⁴ Department of Mathematical Sciences, University of Nevada, Las Vegas, NV, monika.neda@unlv.edu

⁵ Department of Mathematics, University of Pittsburgh, Pittsburgh, PA, ler6@math.pitt.edu

⁶ Department of Mathematics, University of Pittsburgh, Pittsburgh, PA, ius1+@pitt.edu

⁷ Department of Mathematics, University of Pittsburgh, Pittsburgh, PA, trenchea@pitt.edu

Summary. This report presents the mathematical foundation of approximate deconvolution LES models together with the model phenomenology downstream of the theory.

Key words: deconvolution, energy cascade, helicity, MHD

1.1 Introduction

One of the most interesting approaches to generate LES models is via approximate deconvolution or approximate / asymptotic inverse of the filtering operator G . Approximate deconvolution models (ADM) are systematic (rather than ad hoc). See, for example, [1, 2, 55, 57, 56, 58] for the work of Stolz, Adams, Kleiser and coworkers and [23, 24, 25, 26] for Geurts' work. They can achieve high theoretical accuracy and shine in practical tests; they contain few or no fitting/tuning parameters. The ADM approach has thus proven itself to be very promising with fundamental reasons for their effectiveness, which we discuss herein. The basic (and *ill-posed*) problem of approximate de-convolution is: (Section 1.2)

given \bar{u} (+ *noise*) find *useful* approximations $D(\bar{u})$ of u
that lead to *accurate* and *stable* LES models.

Indeed, given an approximate deconvolution operator D with accuracy $O(\delta^\alpha)$:

$$\phi = D\bar{\phi} + O(\delta^\alpha) \text{ for smooth functions } \phi$$

the closure problem can be solved approximately to accuracy $O(\delta^\alpha)$ by

$$\overline{u\bar{u}} \leftarrow \overline{D(\bar{u})D(\bar{u})} \quad (+ O(\delta^\alpha)).$$

With the above closure approximation inserted in the SFNSE and adding a time relaxation term $\chi(w - D(\bar{w}))$ we obtain an ADM given by

$$w_t + \nabla \cdot (\overline{D(w)D(w)}) - \nu \Delta w + \nabla q + \chi(w - D(\bar{w})) = \bar{f}(x), \text{ and } \nabla \cdot w = 0.$$

The key to an ADMs physical fidelity and robust mathematical theory is having the correct global energy balance. In Section 1.3 we show that provided D and $I - D$ are SPD, with the weighted norms $(v, w)_D := (D_N v, w)_{L^2(\Omega)}$ and $\|w\|_D^2 := (w, w)_D$, we have

$$\begin{aligned} & \frac{1}{2} [\|w(T)\|_D^2 + \delta^2 \|\nabla w(T)\|_D^2] + \int_0^T \nu \|\nabla w(t)\|_D^2 + \nu \delta^2 \|\Delta w(t)\|_D^2 + \chi(w - D(\bar{w}), w)_D dt \\ & = \frac{1}{2} [\|\bar{u}_0\|_D^2 + \delta^2 \|\nabla \bar{u}_0\|_D^2] + \int_0^T (f, w(t))_D dt. \end{aligned}$$

* Partially supported by NSF Grant DMS 0508260

This energy equality is the key to both the rigorous theory (Section 1.3) and turbulent phenomenology (Section 1.4). In fact, *its derivation gives a roadmap to development of both for LES models for coupled NS systems* (we develop the theory for MHD turbulence in Section 1.6). A correct prediction of turbulent flow means getting the energy balance and rotational structures correct. In the large, this means the ADMs energy and helicity statistics (an open problem for rigorous analysis). Kraichnan's phenomenology (Section 1.4) predicts correctness of the ADM statistics over the resolved scales:

$$\widehat{E}(k) \simeq \alpha_{model} \varepsilon_{model}^{2/3} k^{-5/3}, \quad \widehat{H}(k) \simeq C_{model} \gamma_{model} \varepsilon_{model}^{-1/3} k^{-5/3}, \quad \text{for } k \leq \frac{\pi}{\delta}.$$

This theory is mostly developed in the absence of boundaries. In the presence of boundaries the difficult problems of commutativity, near wall modeling and filtering through a boundary still arise. These problems have motivated reconsideration of the oldest ideas in fluid dynamics: using simple regularizations of the NSE instead of complex models. We have shown that deconvolution can produce dramatic improvement in NSE regularizations as well. Two are presented in Section 1.5: the Leray deconvolution regularization and the deconvolution NS-alpha regularization.

Overall, we see that strong stability + high accuracy leads to good things in LES models. The ADM approach is one path (of several) of obtaining both simultaneously. We also believe that deconvolution ideas have strong independent value and can be used to improve most (or all) LES models and NSE regularizations.

1.2 Approximate Deconvolution

The basic problem in approximate deconvolution is:

$$\text{given } \bar{\mathbf{u}} + \text{noise, find } \bar{\mathbf{u}} \text{ approximately.} \quad (1.1)$$

Typically, the averaging operator is not stably invertible, so various approximate deconvolutions are necessary:

1. The van Cittert deconvolution operator.

The van Cittert method of approximate deconvolution, see [8], constructs a family D_N of inverses to G using N steps of fixed point iterations.

Algorithm 1.2.1 [*van Cittert Algorithm*]: Given an averaging operator G , choose $\mathbf{u}_0 = \bar{\mathbf{u}}$. For $n = 0, 1, 2, \dots, N-1$ perform $\mathbf{u}_{n+1} = \mathbf{u}_n + \{\bar{\mathbf{u}} - G\mathbf{u}_n\}$. Set $D_N \mathbf{u} := \mathbf{u}_N$.

A mathematical theory of the van Cittert deconvolution operator and LES models is developing [1, 7, 20] and [35]. For example, it is known that if G is SPD then $D_N : L^2(Q) \rightarrow L^2(Q)$ is a bounded operator. For $N = 0, 1$, and 2 the transfer function of D_N is $\widehat{D}_0 = 1$, $\widehat{D}_1 = 2 - \frac{1}{k^2+1} = \frac{2k^2+1}{k^2+1}$, and $\widehat{D}_2 = 1 + \frac{1}{k^2+1} + \left(\frac{k^2}{k^2+1}\right)^2$, Figure 1.1. (a).

2. The Accelerated van Cittert deconvolution operator.

Relaxation parameters can be included in Algorithm 1.2.1 at little additional computational cost.

Algorithm 1.2.2 [*Accelerated van Cittert Algorithm*]: Given relaxation parameters ω_n , choose $\mathbf{u}_0 = \bar{\mathbf{u}}$. For $n = 0, 1, 2, \dots, N-1$ perform $\mathbf{u}_{n+1} = \mathbf{u}_n + \omega_n \{\bar{\mathbf{u}} - G\mathbf{u}_n\}$. Set $D_N^\omega \mathbf{u} := \mathbf{u}_N$.

Proposition 1. Let the averaging operator be the differential filter $G\varphi := (-\delta^2 \Delta + I)^{-1} \varphi$. If the relaxation parameters ω_i are positive, for $i = 0, 1, \dots, N$, then the Accelerated van Cittert deconvolution operator $D_N^\omega : L^2(Q) \rightarrow L^2(Q)$ is symmetric positive definite.

Proof. The proof follows from [[42], Lemma 3.2].

The transfer functions of D_N^ω for $N = 1$ and 2 are $\widehat{D}_1^\omega = 1 + \omega_0 \frac{k^2}{k^2+1}$, $\widehat{D}_2^\omega = 1 + (\omega_0 + \omega_1) \frac{1}{k^2+1} - \omega_0 \omega_1 \frac{1}{(k^2+1)^2}$. Optimal values of the relaxation parameters ω_i , for $i = 0, 1, 2, 3, 4$ were calculated in [42], Table 1. With these values, in Figure 1.1. (b) we plot D_N^ω for $N = 1$ and 2 and exact deconvolution.

The graphs of the transfer functions have high order contact at 0. Thus D_N and D_N^ω lead to a very accurate solution of the deconvolution problem.

3. Tichonov regularization deconvolution operator.

Given $\bar{\mathbf{u}}$ and $1 > \mu > 0$, since G is SPD, an approximate solution to the deconvolution problem (1.1) can be calculated as the unique minimizer in $L^2(Q)$ of the functional

$$F_\mu(\mathbf{v}) = \frac{1}{2}(G\mathbf{v}, \mathbf{v}) - (\bar{\mathbf{u}}, \mathbf{v}) + \frac{\mu}{2}(\mathbf{v} - G\mathbf{v}, \mathbf{v}).$$

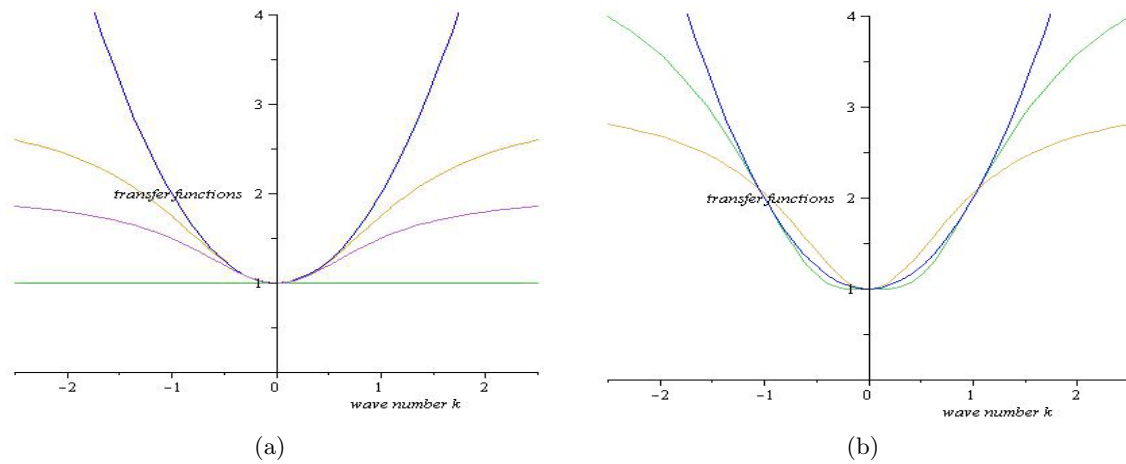


Fig. 1.1. (a) Transfer functions of G^{-1} and D_N ($N=0,1,2$); (b) Exact and Accelerated D_N ($N=1,2$)

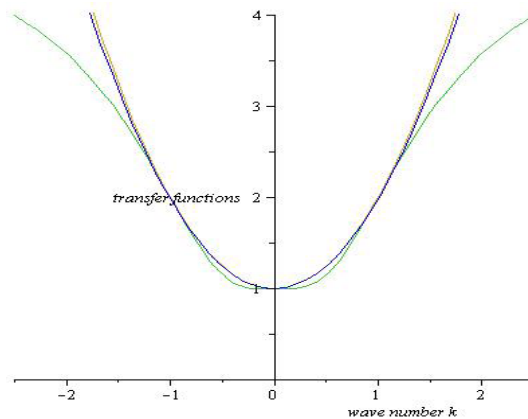


Fig. 1.2. Exact and Tichonov Deconvolution ($\mu = 0.1, 0.01$)

The resulting family of Tichonov regularization deconvolution operators is

$$D_\mu = ((1 - \mu)G + \mu I)^{-1}. \quad (1.2)$$

The family of operators D_μ has the following properties, [53]

- for any $\mu > 0$, D_μ is a bounded SPD operator,
- $\lim_{\mu \rightarrow 0} D_\mu \bar{\varphi} = \bar{\varphi}$ for all $\bar{\varphi} \in L^2(Q)$.

The transfer function of the Tichonov deconvolution operator is

$$\hat{D}_\mu = \frac{1 + k^2}{1 + \mu k^2}.$$

To plot \hat{D}_μ , we consider $\mu = 0.1$, and 0.01 . Figure 1.2 shows that as $\mu \rightarrow 0$, D_μ becomes very accurate.

1.3 Theory of Approximate deconvolution models

In the absence of boundaries, the exact SFNSE can be rewritten as

$$\bar{u}_t + \nabla \cdot (\overline{D(\bar{u})D(\bar{u})}) - \nu \Delta \bar{u} + \nabla \bar{p} + \nabla \cdot (\overline{uu - D(\bar{u})D(\bar{u})}) = \bar{f}(x), \text{ and } \nabla \cdot \bar{u} = 0. \quad (1.3)$$

An LES model results from dropping the residual stress / consistency error $uu - D(\bar{u})D(\bar{u})$. The smaller the consistency error, the closer the model is to the exact SFNSE and (hopefully) the closer the model's solution is to the exact \bar{u} . The residual stress / consistency error, $\overline{uu - D(\bar{u})D(\bar{u})}$, is directly related to the deconvolution error $u - D(\bar{u})$ since

$$\overline{uu - D(\bar{u})D(\bar{u})} = \overline{[u - D(\bar{u})]u} + \overline{D(\bar{u})[u - D(\bar{u})]}.$$

Thus, the more accurately the deconvolution problem can be solved, the more accurately (on the large scales) the closure problem is approximated.

The approximate deconvolution model results from dropping the residual stress tensor τ on the right-hand side of the SFNSE (1.3) and adding the high order relaxation term $\chi(w - D(\bar{w}))$. Thus, this tensor represents the model consistency error.

1.3.1 The Zeroth Order Model

The zeroth order van Cittert operator is $D = I$ or, equivalently, the simple approximation $\phi = \bar{\phi} + O(\delta^2)$. This gives the simplest $N = 0$ closure model

$$\overline{uw} \leftarrow \overline{u} \overline{w} + O(\delta^2)$$

and yields the zeroth order ADM:

$$w_t + \nabla \cdot (\overline{w} w) - \nu \Delta w + \nabla q = \bar{f}(x), \text{ and } \nabla \cdot w = 0. \quad (1.4)$$

The zeroth order model is not of sufficient accuracy for practical computations. It has, however, proven to be an important, even breakthrough test bed of mathematical ideas in LES. All the key mathematical results for approximate deconvolution models were first proven for the zeroth order model and the proofs in the general case were based on the ideas developed for it. We start with the most important example.

Theorem 1. (from [33]) *Consider (1.4) with L -periodic boundary conditions and the initial condition $w(x, 0) = \bar{u}_0(x)$.*

$$\bar{\Phi} = A^{-1} \Phi, \quad A = -\delta^2 \Delta + 1.$$

Let the averaging operator be the differential filter: Then, weak solutions to the zeroth order model exist uniquely and satisfy the energy equality:

$$\frac{1}{2} [\|w(t)\|^2 + \delta^2 \|\nabla w(t)\|^2] + \int_0^t [\nu \|\nabla w(t')\|^2 + \nu \delta^2 \|\Delta w(t')\|^2] dt' = \frac{1}{2} \|u_0(t)\|^2 + \int_0^t (f(t'), w(t')) dt'.$$

Proof. (Sketch) The key to the model, like the NSE, is to make the nonlinear term vanish by an appropriate choice of test function. In the zeroth order model's case we observe

$$(\nabla \cdot (\overline{w} w), Aw) = (A^{-1} \nabla \cdot (w w), Aw) = (\nabla \cdot (w w), w) = (\text{as for the NSE case}) = 0.$$

Thus, the key to the model is taking the inner product of (1.4) with Aw . Since

$$(\nabla q, Aw) = (q, \nabla \cdot Aw) = (q, A \nabla \cdot w) = 0,$$

we have

$$(w_t, Aw) + (\nabla \cdot (\overline{w} w), Aw) - \nu (\Delta w, Aw) + (\nabla q, Aw) = (\bar{f}(t), Aw). \quad (1.5)$$

Integrating by parts each term gives

$$\frac{1}{2} \frac{d}{dt} [(w, w) + \delta^2 (\nabla w, \nabla w)] + [\nu (\nabla w, \nabla w) + \delta^2 (\Delta w, \Delta w)] = (f(t), w).$$

This energy estimate has many important consequences.

- Existence, uniqueness and regularity of strong solutions, [34].
- Correct prediction of turbulent flow statistics for homogeneous, isotropic turbulence through the resolved scales and accelerated attenuation of energy thereafter, [41].
- Convergence (modulo a subsequence) of the models solution as the averaging radius $\delta_j \rightarrow 0$ to a weak solution of the Navier Stokes equations, [34].
- Optimal estimates of the model error ($\|\bar{u}_{NSE} - w_{LES}\|$) is bounded by the model's consistency error (or residual stress), [34].
- Exact conservation of a model energy in the appropriate case (zero viscosity and body force). This implies in particular, global existence for the zeroth order Euler-deconvolution model obtained by setting $\nu = 0$, see [34, 33].
- A first result that the zeroth order model does not induce non-physical vortical structures, and correct prediction of vorticities for low regularity flow data, see [34, 44].

The problem of non-periodic boundaries can be vexing because it includes the issues of filtering through a boundary and finding effective boundary conditions for (non-local) flow averages or near-wall laws. In [MM05] both important problems were resolved by a clean and computationally attractive formulation of averaging that seems to extend to the general N^{th} order model. Also, a complete numerical analysis of variational discretizations of the model was performed, i.e., the problem of numerical errors in the model was resolved. Interestingly, stability was delicate but with the correct filtering: *no additional numerical or model dissipation is needed for a stable simulation*. With other seemingly natural filtering procedures, the model's discrete kinetic energy was seen to blow up in finite time.

1.3.2 Energy balance of general ADMs

The extension to the van Cittert family was accomplished by Dunca [19] and Dunca and Epshteyn [20]. With $D = D_N$ and $\chi = 0$, they showed

$$\frac{1}{2} [\|w(T)\|_D^2 + \delta^2 \|\nabla w(T)\|_D^2] + \int_0^T \nu \|\nabla w(t)\|_D^2 + \nu \delta^2 \|\Delta w(t)\|_D^2 dt = \frac{1}{2} [\|\bar{u}_0\|_D^2 + \delta^2 \|\nabla \bar{u}_0\|_D^2] + \int_0^T (f, w(t))_D dt. \quad (1.6)$$

The main differences between $N = 0$ and $n \geq 1$ cases are that the consistence error is very high: $C(\text{Re})\delta^{2N+2}$ vs. $O(\delta^2)$ and the while the zeroth order model is exactly Galilean invariant, [33], while the N^{th} model is Galilean invariant to $O(\delta^{2N+2})$.

Beyond van Cittert deconvolution (above), current research, e.g., Stanculescu [53], investigates general deconvolution models. Let D denote an approximate deconvolution operator, so that $\|D\|_{L(L^2(\Omega) \rightarrow L^2(\Omega))} < \infty$ and

$$\|D\|_{L(L^2(\Omega) \rightarrow L^2(\Omega))} < \infty \text{ and } D \bar{\phi} \simeq \phi \text{ in some useful sense.}$$

The associated *base* approximate deconvolution is

$$w_t + \nabla \cdot (\overline{Dw Dw}) - \nu \Delta w + \nabla q = \bar{f}(x), \text{ and } \nabla \cdot w = 0. \quad (1.7)$$

Like the $N = 0$ case, the consistency error / residual stress tensor of the base ADM is

$$\tau(u, u) = D(u) D(u) - uu.$$

Finding the energy balance of the general model depends upon: given w , construct an associated function $\Phi(w)$ with

$$(\nabla \cdot (\overline{Dw Dw}), \Phi(w)) = \dots = (v \cdot \nabla v, v) = 0.$$

Taking $\Phi(w) = ADw$ we find (with $v = D(w)$) from (1.7)

$$\begin{aligned} (\nabla \cdot (\overline{Dw Dw}), ADw) &= (A^{-1} \nabla \cdot (Dw Dw), ADw) = (\nabla \cdot (D(w)D(w)), D(w)) = \\ &= (v \cdot \nabla v, v) = (\text{as for the NSE case}) = 0. \end{aligned}$$

This gives, following the zeroth order case, the energy estimate (1.6) since we have

$$(w_t, ADw) - \nu(\Delta w, ADw) = (\bar{f}(x, t), ADw). \quad (1.8)$$

This is deconvolution weighted version of the same energy estimate as the $N = 0$ case (compare (1.6) with Theorem 1). If the operators involved commute (as is expected in the periodic case) and the operator D is SPD then this just represents a weighting of the usual L^2 norm and inner product.

We thus have the fundamental compatibility conditions that

$$\Delta, A, D \text{ commute, and } D \text{ is SPD.}$$

As an example, in the periodic case the Laplacian and the Stokes operator coincide, apart from their domains of definition. Both the differential filter A and the van Cittert approximate deconvolution operators are functions of the Laplacian (specifically, $D = f(A)$ and $A = g(\Delta)$). Thus all three operators commute. The assumption that D is SPD is thus the essential condition.

Proposition 2. *Let G be the differential filter $G = A^{-1}$ where $A = -\delta^2 \Delta + 1$. Then, the van Cittert approximate deconvolution operator is symmetric positive definite.*

Proof. Both A^{-1} and $(I - A^{-1})$ are SPD. For example, $(I - A^{-1})$ is a SPD since

$$(\phi, (I - A^{-1})\phi) = (\text{letting } \psi = A^{-1}\phi) = \delta^4 \|\Delta\psi\|^2 + \delta^2 \|\nabla\psi\|^2 > 0$$

for $\phi \neq 0$. The operator D_N can thus be written as a sum of SPD operators:

$$D_N = \sum_{n=0}^N (I - A^{-1})^n$$

When D is SPD, we can work with associated weighted norms.

Using weighted norms, integrating by parts each term in the energy equation gives

$$\frac{1}{2} \frac{d}{dt} [\|v\|_D^2 + \delta^2 \|\nabla v\|_D^2] + [\nu \|\nabla v\|_D^2 + \nu \delta^2 \|\Delta v\|_D^2] = (f(t), w)_D.$$

The above clearly identifies the ADM energy and energy dissipation rate. The ADM kinetic energy, conserved exactly if $\nu = f = 0$, and energy dissipation rate are given by

$$E_{ADM}(w) = \frac{1}{2} \frac{1}{|\Omega|} [\|w\|_D^2 + \delta^2 \|\nabla w\|_D^2], \quad \varepsilon_{ADM}(w) := \frac{\nu}{|\Omega|} \|\nabla w\|_D^2 + \frac{\nu \delta^2}{|\Omega|} \|\Delta w\|_D^2.$$

These are the essential ingredients (together with complementing mathematical technicalities) of the following result of Stanculescu [53].

Theorem 2 (ADM Energy Equality). *Suppose that Δ, A, D commute, D is SPD. Then, a unique strong solution of the general ADM exists. Further, the following energy equality holds*

$$E_{ADM}(w)(t) + \int_0^t \varepsilon_{ADM}(w)(t') dt' = E_{ADM}(w)(0) + \int_0^t \frac{1}{|\Omega|} (f, w)(t') dt'.$$

From the energy equality, mathematical and physical theories of the approximate deconvolution model with SPD deconvolution operators parallel the zeroth order model. For example, the following results are known.

- **The Leray theory of the model:** Existence, uniqueness and regularity of strong solutions, Layton and Lewandowski [33, 34], Dunca [19], Dunca and Epstein [20], Stanculescu [53], Berselli, Iliescu and Layton [7] and convergence modulo a subsequence to a weak solution of the Navier-Stokes equations:

$$w_{ADM} \rightarrow u_{NSE}, \text{ as } \delta_j \rightarrow 0.$$

- **High Accuracy:** High accuracy for the large scales. For van Cittert deconvolution:

$$\max_{[0, T]} \|\bar{u} - w\|^2 + \int_0^T \nu \|\nabla(\bar{u} - w)\|^2 dt' \leq C(u, \text{Re}) \delta^{4N+4}.$$

- **Physical fidelity:** correct prediction of turbulent flow statistics. Model phenomenology predicts an energy cascade and helicity with the correct statistics through the resolved scales and an accelerated energy attenuation thereafter, ([39, 40, 37], see also Section 1.4):

$$\widehat{E}(k) \approx C \langle \varepsilon_{model} \rangle^{\frac{2}{3}} k^{-\frac{5}{3}}, \quad \text{and} \quad \widehat{H}(k) \approx C \langle \gamma_{model} \rangle \langle \varepsilon_{model} \rangle^{-1/3} k^{-5/3} \text{ over } k_{\min} \leq k \leq 1/\delta.$$

1.4 Phenomenology of Approximate deconvolution models

In 1961 helicity's inviscid invariance was discovered [46]. (See also [45]). Helicity is a *rotationally* meaningful quantity that can be checked for accuracy in a simulation. There is considerable evidence that both energy and helicity exhibit cascades and the details of their respective cascades are intertwined, e.g. [4]. Recent theoretical studies, which have been experimentally confirmed by [9], have suggested that for homogeneous, isotropic turbulence averaged fluid velocities exhibit a joint energy and helicity cascade through the inertial range of wave numbers given by

$$E(k) = C_E \epsilon^{2/3} k^{-5/3}, \quad H(k) = C_H \gamma \epsilon^{-1/3} k^{-5/3},$$

where k is wave number, ϵ the time averaged energy dissipation rate, γ the time averaged helicity dissipation rate and C_E, C_H constants of proportionality for energy and helicity respectively, see [10, 11, 18].

1.4.1 Energy Cascade of Approximate deconvolution models

The correctness of an LES model is prediction of Energy cascades of LES models were first studied by Muschinsky [47], and later by Holm, Olson and Titi [21] followed by [39, 40] for ADMs. If we set $\chi = 0$ and apply A to the ADM it becomes:

$$\frac{\partial}{\partial t} [\mathbf{w} - \delta^2 \Delta \mathbf{w}] + D_N(\mathbf{w}) \cdot \nabla D_N(\mathbf{w}) - \nu [\Delta \mathbf{w} - \delta^2 \Delta^2 \mathbf{w}] + \nabla P = \mathbf{f}, \quad \text{in } \Omega \times (0, T).$$

Since D_N is spectrally equivalent to the identity (uniformly in k , δ , nonuniformly in N) the nonlinear interaction $D_N(\mathbf{w}) \cdot \nabla D_N(\mathbf{w})$ (like those in the NSE) will pump energy from large scales to small scales. The viscous terms in the above equation will damp energy at the small scales (more strongly than in the NSE in fact). Lastly, when $\nu = 0$, $f \equiv 0$ the model's kinetic energy is exactly conserved.

$$E_{model}(\mathbf{w})(t) = E_{model}(\mathbf{w}_0).$$

Thus, the family of ADMs satisfies all the requirements for the existence of a Richardson - like energy cascade for E_{model} . We thus proceed to develop a similarity theory for ADM's (paralleling the K-41 theory of turbulence) using the Π -theorem, see e.g. [17].

The units of a variable will be denoted by $[\cdot]$. Select the variables:

- E_{model} - time averaged energy spectrum of model with $[E_{model}] = length^3 time^{-2}$,
- ε_{model} - time averaged energy dissipation rate of the model with $[\varepsilon_{model}(k)] = length^2 time^{-3}$,
- k - wave-number with $[k] = length^{-1}$ and
- δ - averaging radius with $[\delta] = length$.

Choosing primary dimensions *mass*, *length* and *time*, form 2 dimensionless ratios, Π_1 and Π_2 . Choosing ε and k for the repeating variables we obtain $\Pi_1 = \varepsilon_{model}^a k^b E_{model}$ and $\Pi_2 = \varepsilon_{model}^c k^d \delta$ for some a, b, c, d real numbers. Equating the exponents of the corresponding dimensions in both dimensionless groups and applying the Π -theorem gives

$$E_{model} = \varepsilon_{model}^{2/3} k^{-5/3} f(k\delta).$$

Economy of explanation suggests that $f(\Pi_2) = \alpha_{model}$, (see [40]). In this case we have

$$E_{model}(k) = \alpha_{model} \varepsilon_{model}^{2/3} k^{-5/3}.$$

However, interesting conclusions result from the difference between $E(\mathbf{w})(t)$ and $E_{model}(\mathbf{w})(t)$. Based on Parseval's equality we have $E_{model}(k) = (I + \delta^2 k^2)^{-1} E(k)$ so

$$E(k) = \frac{\alpha_{model} \varepsilon_{model}^{2/3} k^{-5/3}}{1 + \delta^2 k^2}. \quad (1.9)$$

Equation (1.9) gives precise information about how small scales are truncated by the base ($\xi = 0$) ADMs. Indeed, there are two wave-number regions depending on which term in the denominator is dominant: 1 or $\delta^2 k^2$. The transition point is the cutoff wave-number $k = \frac{\pi}{\delta}$. We thus have (Figure 1.3)

$$E(k) \simeq \alpha_{model} \varepsilon_{model}^{2/3} k^{-5/3}, \quad \text{for } k \leq \frac{\pi}{\delta}, \quad E(k) \simeq \alpha_{model} \varepsilon_{model}^{2/3} \delta^{-2} k^{-11/3}, \quad \text{for } k \geq \frac{\pi}{\delta}.$$

Next, we give a summary of the similar explored studies.

- *Kraichnan's dynamic analysis applied to ADM's*. In [40, 37] the dynamical argument of Kraichnan [29] was used to study the non-dimensional function $f(\Pi_2)$. The dynamic argument strongly supports the case $f(\Pi_2) \equiv \text{constant}$.
- *The microscale of ADMs*. In [40], the microscale of the ADMs was shown when $\chi = 0$ to be

$$\eta_{model} \simeq Re^{-\frac{3}{10}} L^{\frac{2}{5}} \delta^{\frac{3}{5}} (N+1)^{-\frac{3}{10}}.$$

- *The joint helicity-energy cascade*. A joint energy and helicity cascade has been shown to exist for homogeneous, isotropic turbulence generated by approximate deconvolution models in [37]. The model's energy and helicity both cascade at the correct $O(k^{-5/3})$ rate for inertial range wave numbers up to the cutoff wave number of $O(\frac{1}{\delta})$, and at $O(k^{-11/3})$ afterward until the model's energy and helicity microscale.
- *Time relaxation*. The above analysis of this section presupposes that the relaxation term in the original model of ADMs is zero. Its effects were studied separately in [41]. Relaxation induces a micro-scale, $\eta_{model} \approx \delta$ and triggers decay of eddies.
- *Other filters*. With the differential filter $(-\delta^2 \Delta + 1)^{-1}$, scales begin to be truncated at $l = O(\delta)$ by an enhanced decay of the energy and helicity of $k^{-11/3}$. The exponent $-11/3$ occurs because the filter decays as k^{-2} . For example, with a Gaussian filter, the cutoff wave-number $k_C = \pi/\delta$.

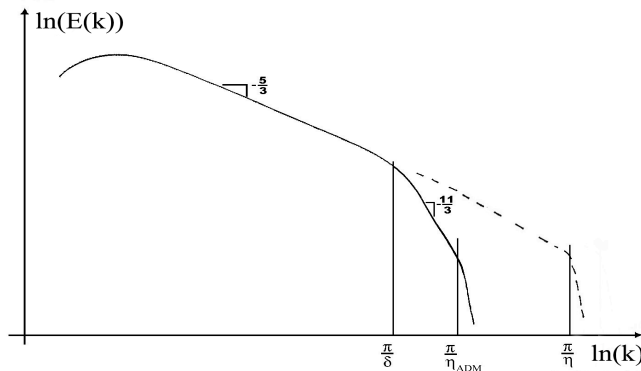


Fig. 1.3. Spectrum of kinetic energy of ADMs

1.5 Deconvolution regularizations of the Navier-Stokes equations

Two regularizations of the (unfiltered) Navier-Stokes equations have recently been proposed and studied. They are the Leray-deconvolution model [36, 38, 50],

$$v_t + D_N \bar{v} \cdot \nabla v + \nabla q - \nu \Delta v = f, \quad \nabla \cdot v = 0, \quad (1.10)$$

and the NS- α -deconvolution model [48, 49],

$$v_t - D_N \bar{v} \times (\nabla \times v) + \nabla q - \nu \Delta v = f, \quad \nabla \cdot D_N \bar{v} = 0. \quad (1.11)$$

Both of these families of models are high-order accurate $O(\delta^{2N+2})$. Also, (1.10) and (1.11) are generalizations of the Leray- α [14, 43] and NS- α models [12, 13, 21, 22, 27], respectively. Although both the Leray- α ($N = 0$ in (1.10)) and NS- α ($N = 0$ in (1.11)) models are well known to have excellent mathematical properties for solution existence, uniqueness and regularity, their accuracy as models of the unfiltered NSE is inadequate for practical computations. From the filtering process, these models' accuracies are reduced to at best $O(\delta^2)$.

1.5.1 The Leray-deconvolution regularization of the NSE

The Leray-deconvolution model (1.10) was proposed in [36], motivated by the low accuracy of the Leray- α model. The Leray regularization [33] has many excellent mathematical properties [14]. However, the Leray- α model has, at best, consistency error of $O(\delta^2)$.

The model studied in [36], called the Leray-deconvolution model, is: let $u_0 \in H_0$, $f \in H_{-1}$ and for fixed $T > 0$ and filtering radius $\delta > 0$, find (v, q) satisfying

$$v \in L^2(0, T; H^1) \cap L^\infty(0, T; H_0), \quad q \in L^2(0, T; L^2_\#), \quad v_t \in L^2(0, T; H_{-1}), \quad (1.12)$$

$$v_t + D_N \bar{v} \cdot \nabla v + \nabla q - \nu \Delta v = D_N \bar{f} \quad (1.13)$$

$$v(0) := v_0 = D_N \bar{u}_0 \quad (1.14)$$

where the $\#$ denotes zero-mean periodic. The consistency error of (1.12)-(1.14) is $O(\delta^{2N+2})$ for smooth NSE solutions, and thus its accuracy can be increased by cutting the filtering radius (and thus the mesh width in a computation), or by holding the filtering radius constant and increasing the order of approximate deconvolution N .

Theorem 3. (from [36]) *The problem (1.12-1.14) admits a unique solution $v \in L^\infty(0, T; H^1) \cap L^2(0, T; H^2)$ which satisfies the energy equality*

$$\|v(t)\|^2 + 2\nu \int_0^t \|\nabla v\|^2 dt' = \|v_0\|^2 + \int_0^t (D_N \bar{f}, v) dt'. \quad (1.15)$$

Theorem 3 shows the desirable mathematical properties of the Leray- α model extend to the family of Leray-deconvolution models of arbitrarily high-order accuracy.

Another advantage of Leray-deconvolution is that it lends itself to efficient computation. The filter-and-deconvolve process can be efficiently treated (as in Baker [5]). By time-extrapolating the first term of the nonlinearity, $O(\Delta t^2)$ accuracy is maintained and only known terms are filtered and deconvolved. This allows van Cittert approximate deconvolution to be applied in a very efficient manner.

Numerical methods for computing solutions to the Leray-deconvolution method were studied in [38]. Using the following discrete definitions for discrete filtering ($A_h^{-1}\phi := \bar{\phi}^h$) and discrete deconvolution (D_N^h) in a finite element space X_h ,

$$\delta^2(\nabla\bar{\phi}^h, \nabla\chi) + (\bar{\phi}^h, \chi) = (\phi, \chi) \quad \forall \chi \in X^h, \quad D_N^h\phi := \sum_{n=0}^N (I - A_h^{-1})^n \phi. \quad (1.16)$$

It is proven in [38] that the consistency of discretely applying approximate deconvolution to a discretely filtered variable is of high order.

Lemma 1. (from [38]) *If X_h is comprised of degree k continuous piecewise polynomials,*

$$\|\phi - D_N^h \bar{\phi}^h\| \leq C(N, \phi)(\delta h^k + h^{k+1} + \delta^{2N+2}). \quad (1.17)$$

This lemma is the key in [38] to showing solutions of trapezoidal finite element schemes for Leray-deconvolution converge at the rate of $O(\Delta t^2 + h^k + h^{2N+2})$, provided sufficient regularity of the true solution and the filtering radius is chosen on the order of the mesh width. This convergence result shows the advantage of using approximate deconvolution, as choosing N to balance the exponents allows for optimal convergence. For $N = 0$ (i.e. Leray- α), optimal convergence cannot be obtained if $k \geq 3$.

In [38], two and three dimensional numerical examples of trapezoidal in time finite element schemes for Leray-deconvolution are given. The 3d computations were done in Matlab using Taylor-Hood tetrahedral elements on an $h = 1/32$ mesh. The 3d tests compared errors for the scheme applied to the NSE and Leray-deconvolution for $N = 0, 1, 2$, and compared conservation properties in the simulations.

Fig. 1.4. The figure below shows L^2 and H^1 error vs time for linear extrapolated Crank-Nicholson finite element schemes with $h = 1/32$, $\text{Re}=5000$, and f computed from the known solution $u = (\cos(2\pi(z+t)), \sin(2\pi(z+t)), \sin(2\pi(x+y+t)))$.

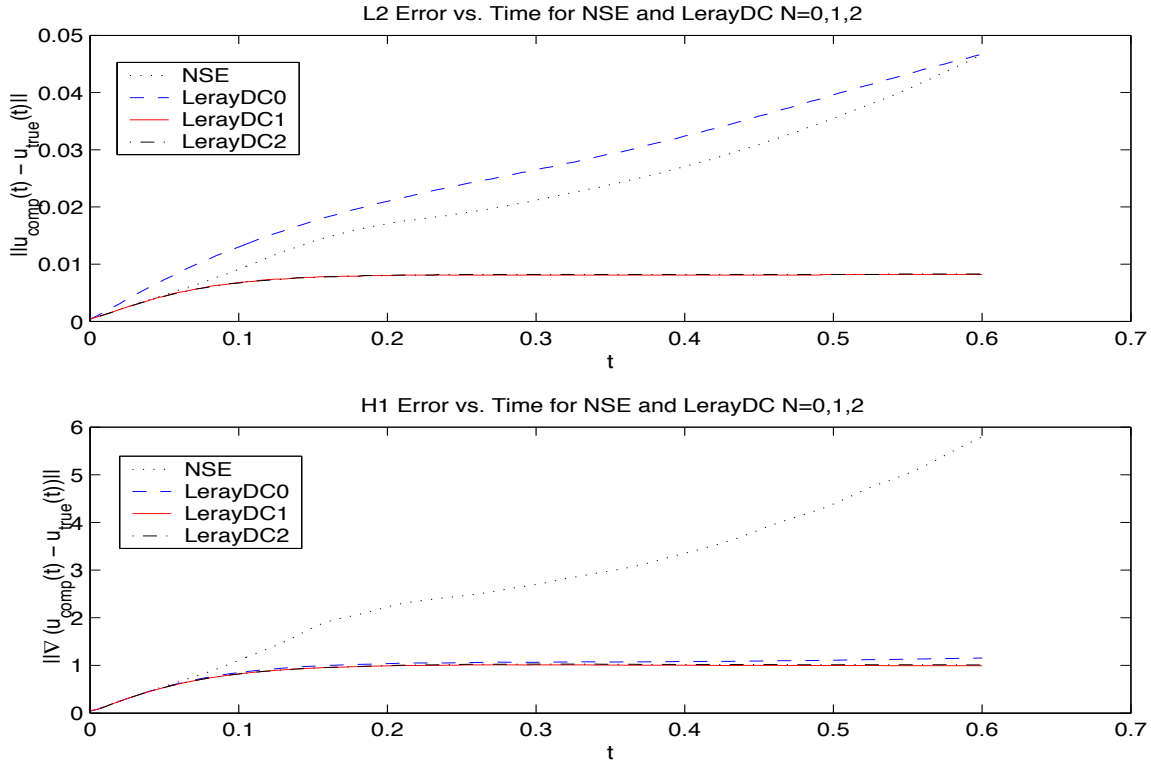
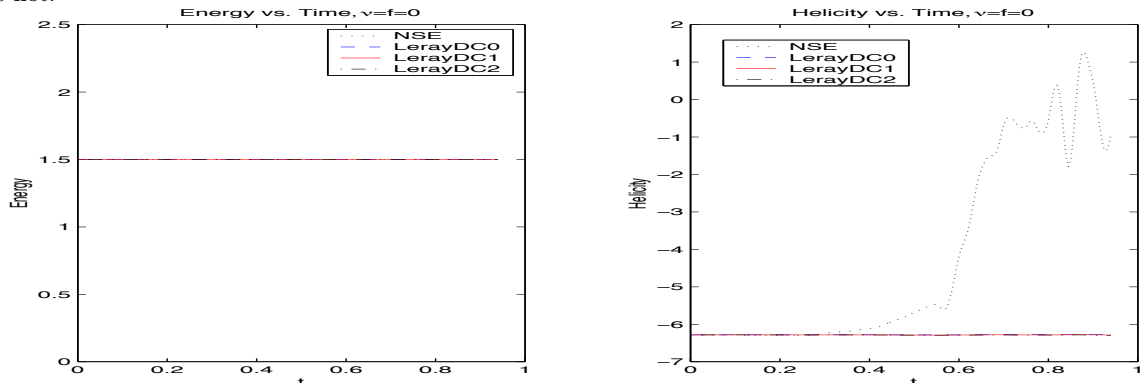


Figure 1.4 shows error versus time for extrapolated trapezoidal finite elements schemes for the NSE, and Leray-deconvolution $N = 0, 1, 2$ on the periodic unit box. The Reynolds number was $\text{Re}=5000$, and f and u_0 were computed from the known solution $u = (\cos(2\pi(z+t)), \sin(2\pi(z+t)), \sin(2\pi(x+y+t)))$. From the figure, it is seen the errors in the Leray-deconvolution models increases at a much slower rate than for the NSE. For the L^2 error, a dramatic decrease in error can be seen in the $N = 1, 2$ models vs. $N = 0$ and NSE.

Figure 1.5 shows, for the extrapolated trapezoidal finite element scheme computations for the NSE and Leray-deconvolution $N = 0, 1, 2$, energy and helicity versus time for a flow with initial condition $u_0 =$

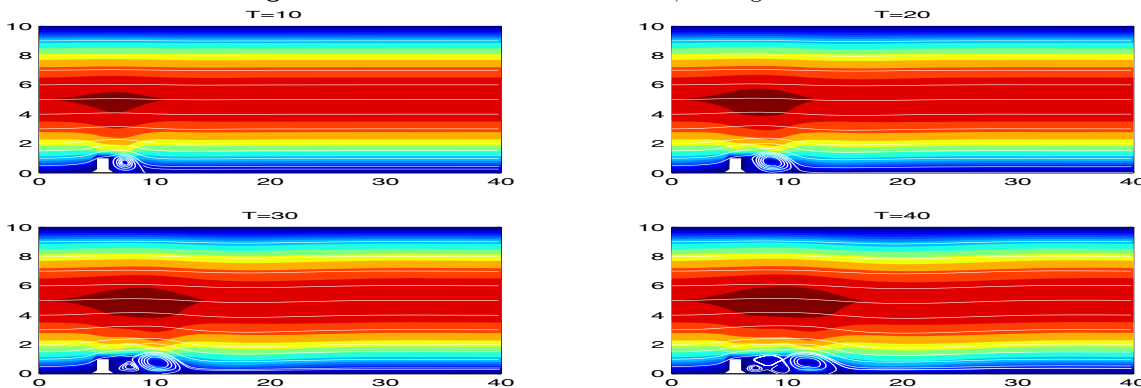
Fig. 1.5. Energy and helicity vs. time of an extrapolated Crank-Nicholson scheme simulation of a flow with initial condition $u_0 = \langle \cos(2\pi z), \sin(2\pi z), \sin(2\pi x + y) \rangle$, $\nu = f = 0$, and $h = 1/32$ for the NSE and LerayDC $N = 0, 1, 2$. Energy is conserved by all the schemes, but LerayDC schemes approximately conserve helicity while the NSE scheme does not.



$\langle \cos(2\pi z), \sin(2\pi z), \sin(2\pi(x + y)) \rangle$, no viscosity or external force ($\nu = f = 0$), and an $h = 1/32$ uniform discretization of the periodic unit cube. In the continuous case, all of these models conserve both energy and helicity under these conditions. For all four models simulations, energy is exactly conserved; this is enforced by the scheme. In the helicity graph, it is seen the Leray-deconvolution models approximately conserve helicity while the NSE simulation does not.

Two dimensional numerical examples are also given in [38] for two dimensional transitional flow ($\nu = 1/600$) over a forward and backward facing step. Figure 1.6 shows the true solution of this problem, run for the Navier-Stokes equations on a very fine mesh (45,138 degrees of freedom), and show the solution at times 10, 20, 30, and 40 seconds. Here it is seen that eddies form behind the step, shed, and new eddies form. Since the purpose of turbulence modeling is to use them with many less d.o.f. than for a DNS, we run the same problem on a much coarser mesh (only 5,845 d.o.f.) for the Leray- α model and for the Leray-deconvolution $N = 2$ models. Figure 1.8 shows the results for the Leray- α model: an eddy forms behind the step and stretches out. This corresponds to the model being too dissipative and the Leray- α model not being sufficient to model the NSE on the same coarse mesh. However, for the Leray-deconvolution $N = 2$ model shown in Figure 1.7 on that same mesh, eddies are seen to break off and new ones form behind the step.

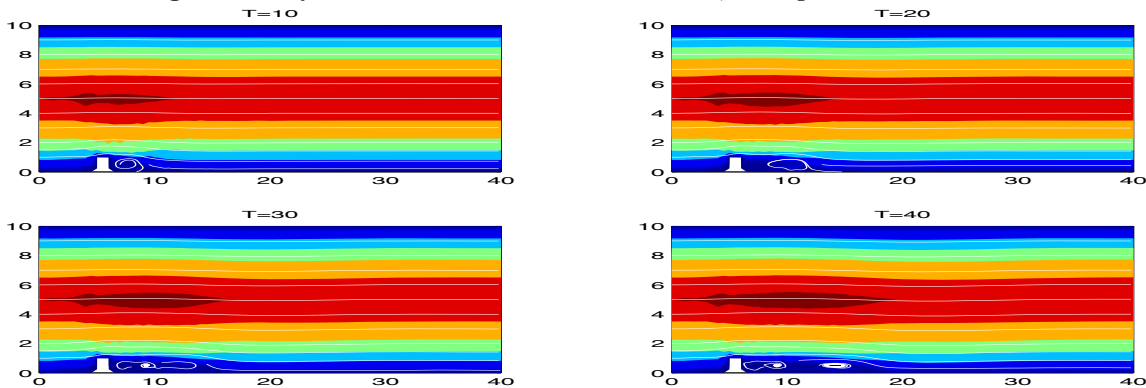
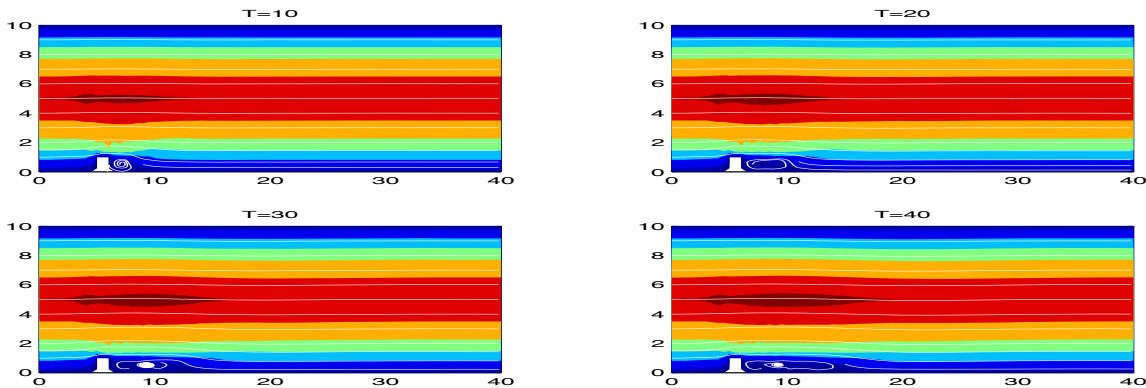
Fig. 1.6. DNS of Navier-Stokes with 45,138 degrees of freedom



The analysis and computations of [36, 38] make a strong case that preserve desirable solution properties, add accuracy, decrease error in computations without decreasing mesh width, and increase physical fidelity.

1.5.2 The NS- α -deconvolution regularization of the NSE

The NS- α -deconvolution model [48] is a helicity-corrected Leray-deconvolution model. One drawback of Leray-deconvolution is an inaccurate treatment of three dimensional rotation. Helicity is as important as energy for understanding three dimensional turbulent flow [45]. Helicity is input at the large scales and cascaded by the nonlinear effects to the small scales where viscous forces drive it to zero [18, 10]. Thus a *physically accurate* turbulence model should do the same; however, the nonlinear effects of the Leray-deconvolution model non-physically create and dissipate helicity [50]. By adding a helicity-correcting term

Fig. 1.7. Leray-deconvolution $N = 2$ simulation on 5,845 degree of freedom mesh**Fig. 1.8.** Leray- α ($N = 0$ Leray-deconvolution) simulation on 5,845 degree of freedom mesh

to Leray-deconvolution (see [48]), a model which treats helicity in a physically accurate manner is recovered: the NS- α -deconvolution model.

Since NS- α -deconvolution has only very recently been proposed, the mathematical theory behind this model has not yet been developed as far as that of the Leray-deconvolution model (but this work is currently underway!). What has been proven is that the NS- α -deconvolution model conserves both a model energy and helicity, and is nonlinearly stable [48]. We formally state these results next, after defining the natural energy and energy dissipation norms of NS- α -deconvolution:

$$\begin{aligned} \|v\|_{E(NS\alpha D)}^2 &:= (v, D_N \bar{v}) = \frac{1}{2} \|\bar{v}\|_D^2 + \frac{\delta^2}{2} \|\nabla \bar{v}\|_D^2 \\ \|v\|_{\epsilon(NS\alpha D)}^2 &:= (\nabla v, \nabla D_N \bar{v}) = \|\nabla \bar{v}\|_D^2 + \delta^2 \|\Delta \bar{v}\|_D^2 \end{aligned}$$

Theorem 4. (From [48]) *Solutions of NS- α -deconvolution on a periodic domain in three dimensions, for $\nu = f = 0$, conserve both energy and helicity: For $T > 0$, and provided sufficient smoothness,*

$$\begin{aligned} E_{NS\alpha D}(T) &= \|v(T)\|_{E(NS\alpha D)} = \|v(0)\|_{E(NS\alpha D)} = E_{NS\alpha D}(0) \\ H(T) &= (v(T), \nabla \times v(T)) = (v(0), \nabla \times v(0)) = H(0) \end{aligned}$$

Theorem 5. *If (v, q) is a solution to (1.11) on a domain Ω given $\nu > 0$, $f \in L^2(0, T; H^{-1}(\Omega))$, and initial velocity $v_0 \in H^1(\Omega)$, then the velocity at time T is bounded by the data:*

$$\|v(T)\|_{E(NS\alpha D)}^2 + \nu \int_0^T \|\nabla v(t)\|_{\epsilon(NS\alpha D)}^2 dt \leq \|v_0\|_{E(NS\alpha D)}^2 + C(N)\nu^{-1} \|f\|_{L^2(0, T; H^{-1})}^2$$

Similar to the accuracy improvement in numerical methods given by Leray-deconvolution ($N \geq 1$) over Leray- α ($N = 0$), improved accuracy in computational schemes for NS- α can be obtained with the use of approximate deconvolution. In [49], a trapezoidal in time finite element numerical scheme for NS- α that preserves both energy and helicity is analyzed, and also generalized to an analogous scheme for NS- α -deconvolution. The convergence analysis for the generalized scheme shows its velocity converges to a NSE solution at the rate of $O(\Delta t^2 + h^k + h^{2N+2})$, where (P_k, P_{k-1}) , $k \geq 2$ elements are used. Hence for Taylor-Hood elements ($k = 2$), optimal convergence is obtained when $N = 0$, but for the higher order elements, using $N = 0$ will give suboptimal convergence rates. However, by increasing N so that $2N + 2 \geq k$, optimal convergence rates can be obtained. Numerical results to test this theory are currently underway, as are experiments to compare the NS- α scheme ($N = 0$) to the NS- α -deconvolution ($N \geq 1$) scheme.

1.6 Complex fluids: the case of MHD turbulence

Magnetically conducting fluids arise in important applications including plasma physics, geophysics and astronomy. In many of these, turbulent MHD (magnetohydrodynamics [3]) flows are typical. The difficulties of accurately modeling and simulating turbulent flows are magnified many times over in the MHD case. They are evinced by the more complex dynamics of the flow due to the coupling of Navier-Stokes and Maxwell equations via the Lorentz force and Ohm's law. The MHD equations are related to engineering problems such as plasma confinement, controlled thermonuclear fusion, liquid-metal cooling of nuclear reactors, electromagnetic casting of metals, MHD sea water propulsion.

The mathematical description of the problem proceeds as follows. Assuming the fluid to be viscous and incompressible, the governing equations are the Navier-Stokes and pre-Maxwell equations, coupled via the Lorentz force and Ohm's law (see e.g. [52]). Let $\Omega = (0, L)^3$ be the flow domain, and $u(t, x), p(t, x), B(t, x)$ be the velocity, pressure, and the magnetic field of the flow, driven by the velocity body force f and magnetic field force $\text{curl } g$. Then u, p, B satisfy the MHD equations:

$$\begin{aligned} u_t + \nabla \cdot (uu^T) - \frac{1}{\text{Re}} \Delta u + \frac{S}{2} \nabla(B^2) - S \nabla \cdot (BB^T) + \nabla p &= f, \\ B_t + \frac{1}{\text{Re}_m} \text{curl}(\text{curl } B) + \text{curl}(B \times u) &= \text{curl } g, \\ \nabla \cdot u = 0, \quad \nabla \cdot B &= 0, \end{aligned} \tag{1.18}$$

in $Q = (0, T) \times \Omega$, with the initial data: $u(0, x) = u_0(x), B(0, x) = B_0(x)$ in Ω , and with periodic boundary conditions (with zero mean). Here Re , Re_m , and S are nondimensional constants that characterize the flow: the Reynolds, the magnetic Reynolds and the coupling number, respectively. For derivation of (1.18), physical interpretation and mathematical analysis, see [16, 32, 51, 28] and the references therein.

If $\bar{\cdot}^{\delta_1}, \bar{\cdot}^{\delta_2}$ denote two local, spacing averaging operators that commute with the differentiation, then averaging (1.18) gives the following non-closed equations for $\bar{u}^{\delta_1}, \bar{B}^{\delta_2}, \bar{p}^{\delta_1}$ in $(0, T) \times \Omega$:

$$\begin{aligned} \bar{u}_t^{\delta_1} + \nabla \cdot (\overline{uu^T}^{\delta_1}) - \frac{1}{\text{Re}} \Delta \bar{u}^{\delta_1} - S \nabla \cdot (\overline{BB^T}^{\delta_1}) + \nabla \left(\frac{S}{2} \overline{B^2}^{\delta_1} + \bar{p}^{\delta_1} \right) &= \bar{f}^{\delta_1}, \\ \bar{B}_t^{\delta_2} + \frac{1}{\text{Re}_m} \text{curl}(\text{curl } \bar{B}^{\delta_2}) + \nabla \cdot (\overline{Bu^T}^{\delta_2}) - \nabla \cdot (\overline{uB^T}^{\delta_2}) &= \text{curl } \bar{g}^{\delta_2}, \\ \nabla \cdot \bar{u}^{\delta_2} = 0, \quad \nabla \cdot \bar{B}^{\delta_2} &= 0. \end{aligned} \tag{1.19}$$

The usual closure problem which we study here arises because $\overline{uu^T}^{\delta_1} \neq \bar{u}^{\delta_1} \bar{u}^{\delta_1}, \overline{BB^T}^{\delta_1} \neq \bar{B}^{\delta_1} \bar{B}^{\delta_1}, \overline{uB^T}^{\delta_2} \neq \bar{u}^{\delta_1} \bar{B}^{\delta_2}$. To isolate the turbulence closure problem from the difficult problem of wall laws for near wall turbulence, we study (1.18) hence (1.19) subject to periodic boundary conditions. The closure problem is to replace the tensors $\overline{uu^T}^{\delta_1}, \overline{BB^T}^{\delta_1}, \overline{uB^T}^{\delta_2}$ with tensors $\mathcal{T}(\bar{u}^{\delta_1}, \bar{u}^{\delta_1}), \mathcal{T}(\bar{B}^{\delta_2}, \bar{B}^{\delta_2}), \mathcal{T}(\bar{u}^{\delta_1}, \bar{B}^{\delta_2})$, respectively, depending only on $\bar{u}^{\delta_1}, \bar{B}^{\delta_2}$ and not u, B . There are many closure models proposed in large eddy simulation reflecting the centrality of closure in turbulence simulation. Calling w, q, W the resulting approximations to $\bar{u}^{\delta_1}, \bar{p}^{\delta_1}, \bar{B}^{\delta_2}$, we are led to considering the following model

$$\begin{aligned} w_t + \nabla \cdot (\overline{ww^T}^{\delta_1}) - \frac{1}{\text{Re}} \Delta w - S \nabla \cdot (\overline{WW^T}^{\delta_1}) + \nabla q &= \bar{f}^{\delta_1}, \\ W_t + \frac{1}{\text{Re}_m} \text{curl}(\text{curl } W) + \nabla \cdot (\overline{Ww^T}^{\delta_2}) - \nabla \cdot (\overline{wW^T}^{\delta_2}) &= \text{curl } \bar{g}^{\delta_2}, \\ \nabla \cdot w = 0, \quad \nabla \cdot W &= 0, \end{aligned} \tag{1.20}$$

subject to $w(x, 0) = \bar{u}_0^{\delta_1}(x), W(x, 0) = \bar{B}_0^{\delta_2}(x)$ and periodic boundary conditions (with zero means).

We show that the LES MHD model (1.20) has the mathematical properties which are expected of a model derived from the MHD equations by an averaging operation and which are important for practical computations using (1.20).

The model considered can be developed for quite general averaging operators, see e.g. [1]. The choice of averaging operator in (1.20) is the differential filter $(-\delta^2 \Delta + I)^{-1}$. (We use different lengthscales for the Navier-Stokes and Maxwell equations). We recall the solenoidal space

$$\mathcal{D}(\Omega) = \{\phi \in C^\infty(\Omega) : \phi \text{ periodic with zero mean, } \nabla \cdot \phi = 0\},$$

and the closures of $\mathcal{D}(\Omega)$ in the usual $L^2(\Omega)$ and $H^1(\Omega)$ norms :

$$H = \{\phi \in H_2^0(\Omega), \nabla \cdot \phi = 0 \text{ in } \mathcal{D}(\Omega)'\}^2, \quad V = \{\phi \in H_2^1(\Omega), \nabla \cdot \phi = 0 \text{ in } \mathcal{D}(\Omega)'\}^2.$$

We define the operator $\mathcal{A} \in \mathcal{L}(V, V')$ by setting

$$\langle \mathcal{A}(w_1, W_1), (w_2, W_2) \rangle = \int_{\Omega} \left(\frac{1}{\text{Re}} \nabla w_1 \cdot \nabla w_2 + \frac{S}{\text{Re}_m} \text{curl } W_1 \text{curl } W_2 \right) dx,$$

for all $(w_i, W_i) \in V$. The operator \mathcal{A} is an unbounded operator on H , with the domain $D(\mathcal{A}) = \{(w, W) \in V; (\Delta w, \Delta W) \in H\}$ and we denote again by \mathcal{A} its restriction to H . We define also a continuous tri-linear form \mathcal{B}_0 on $V \times V \times V$ by setting

$$\begin{aligned} \mathcal{B}_0((w_1, W_1), (w_2, W_2), (w_3, W_3)) &= \int_{\Omega} \left(\nabla \cdot (\overline{w_2 w_1^T}^{\delta_1}) w_3 \right. \\ &\quad \left. - S \nabla \cdot (\overline{W_2 W_1^T}^{\delta_1}) w_3 + \nabla \cdot (\overline{W_2 w_1^T}^{\delta_2}) W_3 - \nabla \cdot (\overline{w_2 W_1^T}^{\delta_2}) W_3 \right) dx \end{aligned}$$

and a continuous bilinear operator $\mathcal{B}(\cdot) : V \rightarrow V$ with

$$\langle \mathcal{B}(w_1, W_1), (w_2, W_2) \rangle = \mathcal{B}_0((w_1, W_1), (w_1, W_1), (w_2, W_2))$$

for all $(w_i, W_i) \in V$.

In terms of $V, H, \mathcal{A}, \mathcal{B}(\cdot)$ we can rewrite (1.20) as

$$\begin{aligned} \frac{d}{dt}(w, W) + \mathcal{A}(w, W)(t) + \mathcal{B}((w, W)(t)) &= (\mathbf{f}^{\delta_1}, \text{curl } \mathbf{g}^{\delta_2}), t \in (0, T), \\ (w, W)(0) &= (\overline{u_0}^{\delta_1}, \overline{B_0}^{\delta_2}), \end{aligned} \tag{1.21}$$

where $(\mathbf{f}, \text{curl } \mathbf{g}) = P(f, \text{curl } g)$, and $P : L^2(\Omega) \rightarrow H$ is the Leray-Hodge projection [15, 54].

Let $(\overline{u_0}^{\delta_1}, \overline{B_0}^{\delta_2}) \in H$, $\mathbf{f}^{\delta_1}, \text{curl } \mathbf{g}^{\delta_2} \in L^2(0, T; V')$. The measurable functions $w, W : [0, T] \times \Omega \rightarrow \mathbb{R}^3$ are called weak solutions of (1.21) if $w, W \in L^2(0, T; V) \cap L^\infty(0, T; H)$, and w, W satisfy

$$\begin{aligned} \int_{\Omega} w(t) \phi dx + \int_0^t \int_{\Omega} \left(\frac{1}{\text{Re}} \nabla w(\tau) \nabla \phi + \overline{w(\tau) \cdot \nabla w(\tau)}^{\delta_1} \phi - S \overline{W(\tau) \cdot \nabla W(\tau)}^{\delta_1} \phi \right) dx d\tau \\ = \int_{\Omega} \overline{u_0}^{\delta_1} \phi dx + \int_0^t \int_{\Omega} \overline{\mathbf{f}(\tau)}^{\delta_1} \phi dx d\tau, \\ \int_{\Omega} W(t) \psi dx + \int_0^t \int_{\Omega} \left(\frac{1}{\text{Re}_m} \nabla W(\tau) \nabla \psi + \overline{w(\tau) \cdot \nabla W(\tau)}^{\delta_2} \psi - \overline{W(\tau) \cdot \nabla w(\tau)}^{\delta_2} \psi \right) dx d\tau \\ = \int_{\Omega} \overline{B_0}^{\delta_2} \psi dx + \int_0^t \int_{\Omega} \text{curl } \overline{\mathbf{g}(\tau)}^{\delta_2} \psi dx d\tau, \end{aligned}$$

$\forall t \in [0, T], \phi, \psi \in \mathcal{D}(\Omega)$.

The main result in [31] states that the weak solution of the MHD LES model (1.20) exists globally in time, for large data and general $\text{Re}, \text{Re}_m > 0$ and that it satisfies an energy equality while initial data and the source terms are smooth enough.

Theorem 6. Let $\delta_1, \delta_2 > 0$ be fixed. For any $(\overline{u_0}^{\delta_1}, \overline{B_0}^{\delta_2}) \in V$ and $(\mathbf{f}^{\delta_1}, \text{curl } \mathbf{g}^{\delta_2}) \in L^2(0, T; H)$, there exists a unique strong solution w, W to (1.20). The strong solution also belongs to $L^\infty(0, T; H^1(\Omega)) \cap L^2(0, T; H^2(\Omega))$ and $w_t, W_t \in L^2((0, T) \times \Omega)$. Moreover, the following energy equality holds for $t \in [0, T]$:

$$E(t) + \int_0^t \epsilon(\tau) d\tau = E(0) + \int_0^t \mathcal{P}(\tau) d\tau,$$

where

$$\begin{aligned} E(t) &= \frac{\delta_1^2}{2} \|\nabla w(t, \cdot)\|_0^2 + \frac{1}{2} \|w(t, \cdot)\|_0^2 + \frac{\delta_2^2 S}{2} \|\nabla W(t, \cdot)\|_0^2 + \frac{S}{2} \|W(t, \cdot)\|_0^2, \\ \epsilon(t) &= \frac{\delta_1^2}{\text{Re}} \|\Delta w(t, \cdot)\|_0^2 + \frac{1}{\text{Re}} \|\nabla w(t, \cdot)\|_0^2 + \frac{\delta_2^2 S}{\text{Re}_m} \|\Delta W(t, \cdot)\|_0^2 + \frac{S}{\text{Re}_m} \|\nabla W(t, \cdot)\|_0^2, \\ \mathcal{P}(t) &= (\mathbf{f}(t), w(t)) + S(\text{curl } \mathbf{g}(t), W(t)). \end{aligned}$$

In the proof we use the semigroup approach proposed in [6] for the Navier-Stokes equations, based on the machinery of nonlinear differential equations of accretive type in Banach spaces. The other results derived for the model (1.20) in [31] concern: (i) *regularity of the solution*, (ii) *error estimates for the model*, (iii) *conservation laws*: the model conserves exactly the approximate physical quantities and (iv) *conservation Alfvén waves*: the model predicts the Alfvén waves correctly. Using a least-squares method, we compute in [30] the radii δ_1, δ_2 defining the averaging differential operators such the solution w, W to (1.20) best approximate any given velocity and magnetic fields u°, B° .

References

1. N.A. Adams and S. Stolz, *Deconvolution methods for subgrid-scale approximation in large-eddy simulation*, Modern Simulation Strategies for Turbulent Flow, R.T. Edwards, 2001.
2. ———, *A subgrid-scale deconvolution approach for shock capturing*, J.C.P. **178** (2002), 391–426.
3. H. Alfvén, *Existence of electromagnetic-hydrodynamic waves*, Nature **150** (1942), 405.
4. J.C. André and M. Lesieur, *Influence of helicity on the evolution of isotropic turbulence at high Reynolds number*, J. Fluid Mech. **81** (1977), 187–207.
5. G. Baker, *Galerkin approximations for the Navier-Stokes equations*, Harvard University, August 1976.
6. V. Barbu and S. S. Sritharan, *Flow invariance preserving feedback controllers for the Navier-Stokes equation*, J. Math. Anal. Appl. **255** (2001), no. 1, 281–307.
7. L.C. Berselli, T. Iliescu, and W. Layton, *Mathematics of large eddy simulation of turbulent flows*, Springer, Berlin, 2006.
8. M. Bertero and B. Boccacci, *Introduction to inverse problems in imaging*, IOP Publishing Ltd., 1998.
9. J. Bourne and S. Orszag, *Spectra in helical three-dimensional homogeneous isotropic turbulence*, Physics Review Letters E **55** (1977), 7005–7009.
10. Q. Chen, S. Chen, and G. Eyink, *The joint cascade of energy and helicity in three dimensional turbulence*, Physics of Fluids **15** (2003), no. 2, 361–374.
11. Q. Chen, S. Chen, G. Eyink, and D. Holm, *Intermittence in the joint cascade of energy and helicity*, Physical Review Letters **90** (2003), 214503.
12. S. Chen, C. Foias, D. Holm, E. Olson, E. Titi, and S. Wynne, *The Camassa-Holm equations as a closure model for turbulent channel and pipe flow*, Phys. Rev. Lett. **81** (1998), 5338–5341.
13. S. Chen, D. Holm, L. Margolin, and R. Zhang, *Direct numerical simulations of the Navier-Stokes alpha model*, Physica D **133** (1999), 66–83.
14. A. Cheskidov, D.D. Holm, E. Olson, and E.S. Titi, *On a Leray- α model of turbulence*, Royal Society London, Proceedings, Series A, Mathematical, Physical and Engineering Sciences **461** (2005), 629–649.
15. A. Chorin and J. Marsden, *A Mathematical Introduction to Fluid Mechanics*, Springer, 2000.
16. T.G. Cowling, *Magnetohydrodynamics*, Interscience Tracts on Physics and Astronomy, New York, 1957.
17. R.L. Daugherty and J.B. Franzini, *Fluid mechanics with engineering applications*, 7th ed., McGraw-Hill, New York, 1977.
18. P. Ditlevsen and P. Guilianani, *Cascades in helical turbulence*, Physical Review E **63** (2001), 036304/1–4.
19. A. Dunca, *Space averaged Navier Stokes equations in the presence of walls*, Ph.D. thesis, University of Pittsburgh, 2004.
20. A. Dunca and Y. Epshteyn, *On the Stolz-Adams deconvolution model for the large eddy simulation of turbulent flows*, SIAM J. Math. Anal. **37** (2006), no. 6, 1890–1902.
21. C. Foias, D.D. Holm, and E. S. Titi, *The Navier-Stokes-alpha model of fluid turbulence*, Physica D **152-153** (2001), 505–519.
22. C. Foias, D.D. Holm, and E.S. Titi, *The three dimensional viscous Camassa-Holm equations, and their relation to the Navier-Stokes equations and turbulence theory*, J. Dynam. Differential Equations **14** (2002), no. 1, 1–35.
23. B. J. Geurts, *Inverse modeling for large eddy simulation*, Phys. Fluids **9** (1997), 3585.
24. B.J. Geurts, *Elements of direct and large eddy simulation*, Edwards Publishing, 2003.
25. B.J. Geurts and D.D. Holm, *Regularization modeling for large eddy simulation*, Physics of fluids **15** (2003), no. 1, L13–L16.
26. ———, *Leray and LANS-alpha modeling of turbulent mixing*, J. of Turbulence **00** (2005), 1–42.
27. J.L. Guermond, J.T. Oden, and S. Prudhomme, *An interpretation of the Navier-Stokes-alpha model as a frame-indifferent Leray regularization*, Phys. D **177** (2003), no. 1-4, 23–30.
28. M.D. Gunzburger, A.J. Meir, and J. Peterson, *On the existence, uniqueness, and finite element approximation of solutions of the equations of stationary, incompressible magnetohydrodynamics*, Math. Comp. **56** (1991), no. 194, 523–563.
29. R. Kraichnan, *Inertial-range transfer in two- and three- dimensional turbulence*, J. Fluid Mech. **47** (1971), 525.
30. A. Labovschii and C. Trenchea, *Identification of averaging radii for the LES in MHD flows*, in preparation.
31. ———, *Large eddy simulation for MHD flows*, Tech. report, University of Pittsburgh, 2007.
32. L. Landau and E. Lifschitz, *Électrodynamique des milieux continus*, Physique théorique, vol. tome VIII, MIR, Moscow, 1969.
33. W. Layton and R. Lewandowski, *A simple and stable scale-similarity model for large eddy simulation: energy balance and existence of weak solutions*, Appl. Math. Lett. **16** (2003), no. 8, 1205–1209.
34. ———, *On a well-posed turbulence model*, Discrete and Continuous Dynamical Systems - Series B **6** (2006), 111–128.
35. ———, *Residual stress of approximate deconvolution large eddy simulation models of turbulence*, J. Turbul. **46** (2006), no. 2, 1–21.
36. ———, *A high accuracy Leray-deconvolution model of turbulence and its limiting behavior*, Analysis and Applications (2007), to appear.
37. W. Layton, C. Manica, M. Neda, and L. Rebholz, *The joint Helicity-Energy cascade for homogeneous, isotropic turbulence generated by approximate deconvolution models*, Tech. report, University of Pittsburgh, <http://www.math.pitt.edu/~techrep/0610.pdf>, 2006.

38. ———, *Numerical analysis of a high accuracy Leray-deconvolution model of turbulence*, Tech. report, TR MATH 06-21, 2006, to appear: Numerical Methods for PDEs, 2007.
39. W. Layton and M. Neda, *The energy cascade for homogeneous, isotropic turbulence generated by approximate deconvolution models*, to appear in: J. Math. Anal. Appl. (2007).
40. ———, *A similarity theory of approximate deconvolution models of turbulence*, J. Math. Anal. Appl. **333** (2007), no. 1, 416–429.
41. ———, *Truncation of scales by time relaxation*, J. Math. Anal. Appl. **325** (2007), no. 2, 788–807.
42. W. Layton and I. Stanculescu, *K-41 optimized approximate deconvolution models*, to appear in: International Journal of Computing Science and Mathematics (2007).
43. J. Leray, *Essay sur les mouvements plans d'une liquide visqueux que limitent des parois*, J. Math. Pur. Appl., Paris Ser. IX **13** (1934), 331–418.
44. R. Lewandowski, *Vorticities in a LES model for 3D periodic turbulent flows*, Journ. Math. Fluid. Mech. **8** (2006), 398–422.
45. H.K. Moffatt and A. Tsinober, *Helicity in laminar and turbulent flow*, Annual review of fluid mechanics, Vol. 24, Annual Reviews, Palo Alto, CA, 1992, pp. 281–312.
46. J.J. Moreau, *Constantes d'unilote tourbillonnaire en fluide parfait barotrope*, C.R. Acad. Aci. Paris **252** (1961), 2810–2812.
47. A. Muschinski, *A similarity theory of locally homogeneous and isotropic turbulence generated by a Smagorinsky-type LES*, J. Fluid Mech. **325** (1996), 239–260.
48. L. Rebholz, *A family of new high order NS-alpha models arising from helicity correction in Leray turbulence models*, submitted (2007), TR MATH 06-19, University of Pittsburgh.
49. L. Rebholz and W. Miles, *Computing NS-alpha with greater physical accuracy and higher convergence rates*, submitted (2007).
50. L.G. Rebholz, *Conservation laws of turbulence models*, J. Math. Anal. Appl. **326** (2007), no. 1, 33–45.
51. M. Sermange and R. Temam, *Some mathematical questions related to the MHD equations*, Comm. Pure Appl. Math. **36** (1983), 635–664.
52. J.A. Shercliff, *A Textbook of Magnetohydrodynamics*, Pergamon, Oxford, 1965.
53. I. Stanculescu, *Existency theory of abstract approximate deconvolution models of turbulence*, Tech. report, University of Pittsburgh, 2007.
54. E. Stein, *Singular Integrals and Differentiability Properties of Functions*, Princeton University Press, 1970.
55. S. Stolz and N.A. Adams, *On the approximate deconvolution procedure for LES*, Phys. Fluids **II** (1999), 1699–1701.
56. S. Stolz, N.A. Adams, and L. Kleiser, *An approximate deconvolution model for large eddy simulation with application to wall-bounded flows*, Phys. Fluids **13** (2001), 997.
57. ———, *The approximate deconvolution model for LES of compressible flows and its application to shock-turbulent-boundary-layer interaction*, Phys. Fluids **13** (2001), 2985.
58. ———, *The approximate deconvolution model for compressible flows: isotropic turbulence and shock-boundary-layer interaction*, Advances in LES of complex flows (R. Friedrich and W. Rodi, eds.), Kluwer, Dordrecht, 2002.